Calibration of Mechanistic-Empirical Models for Flexible Pavements Using the WesTrack Experiment

P. Ullidtz[1], J.T. Harvey[2], B-W. Tsai[3] and C.L. Monismith[3]

Abstract

Calibration of Mechanistic-Empirical (ME) models is an integral part of Caltran's commitment to adopting an ME pavement design method. As a first step, 27 flexible pavement accelerated pavement test sections trafficked by the two California Heavy Vehicle Simulators (HVSs) were used to calibrate the ME models of the software tool CalME. This paper deals with the second step, where the 26 original sections from the WesTrack experiment were used for calibration of CalME models.

Material parameters for calibrating the incremental-recursive models were determined from Falling Weight Deflectometer (FWD) tests and from laboratory tests. The results of the WesTrack experiment, in terms of temperatures at different depths, time of load applications, measured rutting and FWD deflections, and recorded distresses were imported to the CalME database. Each section was then simulated, hour by hour, for the total duration of the experiment. The measured FWD deflections measured at intervals during trafficking at WesTrack were compared to the deflections calculated by CalME, to ensure that the pavement response was predicted reasonably well. The empirical components of the ME models were then calibrated so that the predicted performance would match the measured performance. For prediction of asphalt fatigue a shift factor between laboratory fatigue and in-situ fatigue was determined. For the Fine and Fine Plus mixes the shift factor was found to be approximately 15 (i.e. a load in the laboratory corresponds to 15 loads in-situ) and for the Coarse mix approximately 5, although both values may be somewhat high. For permanent deformation of the asphalt layers the permanent strain determined from Repeated Simple Shear Tests – Constant Height (RSST-CH) in the laboratory should be multiplied by a factor of 90 for Fine and Fine Plus mixes and by 80 for Coarse mixes, to result in the measured downward permanent deformation of the asphalt, in mm. The models used for unbound materials in the HVS experiments were confirmed.

[1] Dynatest International, [2] University of California Pavement Research Center, University of California, Davis, [3] University of California Pavement Research Center, University of California, Berkeley

Introduction

In 2005, the California Department of Transportation (Caltrans) approved an issue memo titled "Adoption of Mechanistic-Empirical (ME) Pavement Design Method", which calls for the adoption of ME pavement design methodology to replace existing pavement design methods, which have been in place since the early 1960s.

The University of California Pavement Research Center (UCPRC) has been supporting the Caltrans effort to adopt ME pavement design by working on a series of tasks. This work is under the technical guidance of the Pavement Standards Team, with the Division of Design in the lead. One of those tasks is to develop and calibrate ME flexible pavement design models in addition to those in the Mechanistic-Empirical Design Guide (MEPDG) developed by NCHRP (1). These models have been incorporated into a draft software program called CalME. CalME allows Caltrans to validate and/or calibrate different mechanistic models of pavement response and different empirical models of pavement performance.

CalME may also be used for Mechanistic-Empirical design of new flexible pavements and for rehabilitation design in California. Deflections and backcalculated layer moduli from Falling Weight Deflectometer (FWD) testing, determined using a companion program called CalBack, may be imported into the CalME database for rehabilitation design. CalME has three levels of design, for new pavements as well as for rehabilitation:

1. Caltrans current methods, the "R-value" method for flexible structures and the "Deflection Reduction" method for overlay design,
2. a "Classical" Mechanistic-Empirical design, largely based on the Asphalt Institute method, using ESALs and a weighted mean annual environmental condition, and
3. an "Incremental-Recursive" method in which the materials properties are updated in terms of damage for each time increment and used (recursively) as input to the next time increment. This approach predicts the pavement conditions at any point in time during the pavement life and was used for the simulations included in this paper.

The validation and calibration of the models in CalME was first performed using performance data from Heavy Vehicle Simulator (HVS) tests completed for Caltrans by the UCPRC between 1995 and 2004. The results of that work are documented in a report which may be downloaded from (2).

The purpose of this paper is to present the results of a validation and calibration study performed by the UCPRC using performance data from the Federal Highways Administration project commonly referred to as "WesTrack".

WesTrack Experiment and Performance Results

Details of the WesTrack experiment and results are available in (3 and 4). Most of the data from WesTrack, including laboratory tests on materials, have been extracted from the database "WesTrack database" (in Access format). The following is a brief summary of the experiment and results to provide background for the modeling of the performance of the WesTrack sections using CalME.

WesTrack refers to an experimental test road facility constructed at the Nevada Automotive Test Center (NATC) near Fallon, Nevada, under the Federal Highway Administration (FHWA) project "Accelerated Field Test of Performance-Related Specifications for Hot-Mix Asphalt Construction". The project was conducted by the WesTrack team, a consortium of seven public- and private-sector organizations lead by the NATC and including Granite Construction Co., Harding Lawson and Associates, Nichols Consulting Engineers, Chtd., Oregon State University, the University of California, Berkeley, and the University of Nevada, Reno.

The WesTrack experiment had two primary objectives. The first was to continue development of performance-related specifications (PRS) for HMA construction by evaluating the impact of deviations in materials and construction properties from design values on pavement performance in a full-scale, accelerated field test. The second was to provide some early field verification of the Superpave® mix design procedures. Because the WesTrack site typically experiences less than 100 mm of precipitation per year and no frost penetration, it was well suited for evaluating the direct effects of deviations of materials and construction properties on performance.

WesTrack was constructed as a 2.9-km oval loop

incorporating twenty-six 70 m long experimental sections on the two tangents. The pavement cross sections consisted of various asphalt concrete mixes placed on a design thickness of 300 mm (12 in.) of aggregate base, with a thick layer of "engineered fill" below, sometimes referred to as the subgrade in this paper. The design thickness of the HMA layer (referred to as asphalt concrete [AC] in this paper) in all sections was 150 mm (6 in.), placed in two 75 mm lifts.

Construction was completed in October 1995; trafficking was carried out between March 1996 and February 1999. During this period, four triple-trailer combinations composed of a tandem axle, Class 8 tractor and a lead semi-trailer followed by two single-axle trailers, operated on the track at a speed of 64 km/h (40 mph), providing 10.3 equivalent single-axle load (ESAL) applications per vehicle pass. The use of autonomous (driver-less) vehicle technology provided an exceptional level of operational safety and permitted loading to occur up to 22 hours per day, 7 days per week.

The experimental variables were in the asphalt concrete mixes, and included asphalt content, in-place (i.e., field-mixed, field-compacted) air void content, and aggregate gradation (Coarse, Fine and Fine Plus); the main performance variables were rut depth and percentage of the wheelpath area with fatigue cracking. Approximately 4.95 million ESALs were applied during the trafficking period. Several original sections failed early in the experiment; they were replaced with a mix design that duplicated the Coarse gradation mix experiment in the original construction, but changed the aggregate source. The replacement sections were constructed in June, 1997 after the application of approximately 2.85 million ESALs. Only the 26 original test sections are considered in this paper. The experiment yielded clearly differentiated levels of permanent deformation and fatigue cracking among the experimental sections.

All of the initial 26 test sections used the same aggregate source and binder in the asphalt concrete. The symbols used in this paper for the three different gradations are: Fine (F), Coarse (C) and Fine Plus (P). The Fine mixes had a Superpave aggregate gradation that passed above the "Restricted Zone" in the Superpave mix design system. The Fine Plus mixes had a gradation that was slightly finer than the Fine gradation. The Coarse mixes had a gradation that passed below the Restricted Zone. For each mix type there were sections with high (H), medium (M) and low (L) asphalt content with target values of

4.7, 5.4 and 6.1 %, respectively for Fine and Fine Plus mixes and 5.0, 5.7 and 6.4 % for the Coarse mix, and with high (H), medium (M) and low (L) air voids content with target values of 4, 8 and 12 %, respectively.

In the naming system used for each section in this paper, "FML" indicates a section with a Fine mix with a medium AC content and a low air voids content (a 1 or 2 following the mix name would indicate whether the section was the first or the second of replicate sections for those cells that had replicates).

Measurements taken during the Westrack experiment and used in this study included Falling Weight Deflectometer (FWD) deflections, pavement temperatures at several depths in the asphalt concrete, and pavement distress condition surveys following the LTPP protocol.

"Classical" Mechanistic-Empirical Models

Details of comparison of the "Classical" ME method with Westrack results are included in the report for this project (5). The following is a brief summary of these results.

The WesTrack project is not very well suited for calibrating "Classical" mechanistic-empirical models, partly because the test was accelerated (less than 3 years) and partly because a number of rather unusual mixes were tested. Nevertheless the rutting and fatigue cracking criteria used in the Asphalt Institute flexible pavement design method are to some extent confirmed by the project.

Had the service life of the pavements been predicted based on moduli back-calculated from FWD tests carried out at the outset of the experiment, the number of loads to 10 mm of downward rut would have generally been predicted quite well. The exceptions were the mixes with a high asphalt content and some of the coarse mixes, where the asphalt layers contribution to the overall rutting was larger than for "usual" pavements.

The number of load applications to 10% cracking would also have been predicted quite well, if the Asphalt Institute criterion were used without modification for volume of binder and voids, so that the effects of volume of binder and volume of voids were accounted for through their effects on the modulus only. The prediction would have been conservative, corresponding to a reliability of 92% with the standard deviation

from the AASHO Road Test (98% with the actual standard deviation of WesTrack).

Incremental-Recursive Models in CalME

Modulus of Asphalt Layers (Master Curve)

The model for intact asphalt concrete modulus versus reduced time was the NCHRP 1-37A model (**Error! Reference source not found.**, MEPDG):

$$\log(E_i) = \delta + \frac{\alpha}{1 + \exp(\beta + \gamma \log(tr))}$$

Equation 1: Asphalt modulus versus reduced time.

where E_i is the modulus in MPa,
tr is reduced time in sec and
α, β, γ, and δ are constants determined from frequency sweep tests.
Log is the logarithm to base 10. Reduced time is found from:

$$tr = lt \times \left(\frac{visc_{ref}}{visc}\right)^{aT}$$

Equation 2: Reduced time as a function of loading time and viscosity.

where lt is the loading time in sec,
$visc$ is the viscosity,
$visc_{ref}$ is the viscosity at a reference temperature, and
aT is a constant.
The viscosity, in cPoise, is found from:

$$\log(\log(visc\,cPoise)) = A + VTS * \log(t_K)$$

Equation 3: Viscosity as a function of temperature.

where t_K is the temperature in ºKelvin and
A and VTS are constants.

Hardening/Aging

Hardening of the asphalt mix may be caused by a reduction in air voids content caused by post compaction and/or by aging (oxidation) of the binder. In CalME a very simple model is used to describe these two effects:

$$E(d1) = E(d0) \times \frac{AgeA \times \ln(d1) + AgeB}{AgeA \times \ln(d0) + AgeB}$$

Equation 4 Hardening of asphalt.

where *E(d)* is the modulus after *d* days,
d0 and d1 are two points in time, in days, and
AgeA and *AgeB* are constants.

Hardening may be limited by a maximum age in days, beyond which no more hardening takes place.

An attempt was made to use the hardening model in the MEPDG. To calculate hardening with time the MEPDG makes use of a model for determining the long time aging of viscosity at the surface, a model for correction of viscosity for the effects of air voids, which includes a model for predicting the change in air voids with time and temperature, and a model for viscosity aging as a function of depth. The models for long term aging of viscosity at the surface and for aging as a function of depth were found to predict large effects on the viscosity at temperatures below 20 ºC but very little effect at higher temperatures. The long term viscosity at a depth of 50 mm hardly changed with aging at temperatures above 20 ºC. For the long term viscosity the relationship between log-log viscosity in cPoise and log temperature in ºK (or ºR) were no longer linear, so that Equation 3 was no longer valid. Even though the viscosity of the binder did not change at high temperatures, the stiffness of the mix did increase at these temperatures, because the viscosity at the reference temperature of 15.4 ºC has an influence on the parameter β in Equation 1. The increase in the mix stiffness was not unreasonable compared to the measured values, but because of the change in viscosity versus temperature relationship which made it impossible to use Equation 3 and because of the inconsistency between the change in viscosity and in mix stiffness, the MEPDG models were not used in this calibration.

Moduli of Unbound Layers

During these and other experiments (6) it has been found that the moduli of unbound materials sometimes vary with the

stiffness of the layers above the layer considered. This may happen as a result of change in stiffness of asphalt layers due to change in temperature, or as a result of increasing damage to the layers. For granular layers this effect is the opposite of what would be expected from conventional understanding of the non-linearity of the granular material stiffness. A decrease in the stiffness of the layers above a granular layer should result in an increase in the bulk stress in the material and, therefore, in an increase in the modulus, whereas the opposite effect is observed. The softening effect due to softening of the layers above is in good agreement with the observation made by Richter (7) based on stiffnesses backcalculated from FWD tests on LTPP Seasonal Monitoring sections, which showed that the moduli of granular layers tend to decrease with increasing bulk stress. An explanation for this could be the confining effect of the layers above. This is illustrated in (2) through a calculation with the Distinct Element Method.

To allow for this effect in CalME, the stiffness of each unbound layer was modeled as a function of the bending stiffness of the layers above it:

$$E = Eo \times \left(1 - \left(1 - S/S_{ref}\right) \times \textit{Stiffness factor}\right), \textit{with}$$

$$S = \left(\sum_{1}^{n-1} h_i \times \sqrt[3]{E_i}\right)^3$$

Equation 5: Modulus of each unbound layer as a function of the bending stiffness of the layers above it.

where Eo is the modulus (of layer n) at the reference stiffness,
S is the combined stiffness of the layers above layer n,
S_{ref} is the reference stiffness (a value of 3500^3 was used here),
h_i is the thickness of layer i in mm, and
E_i is the modulus of layer i in MPa.
The *Stiffness factor* was determined from regression analyses of moduli backcalculated from FWD tests. An example from the first FWD test series on all of the WesTrack test sections is shown in Figure 1.

Moduli as function of stiffness of layers above
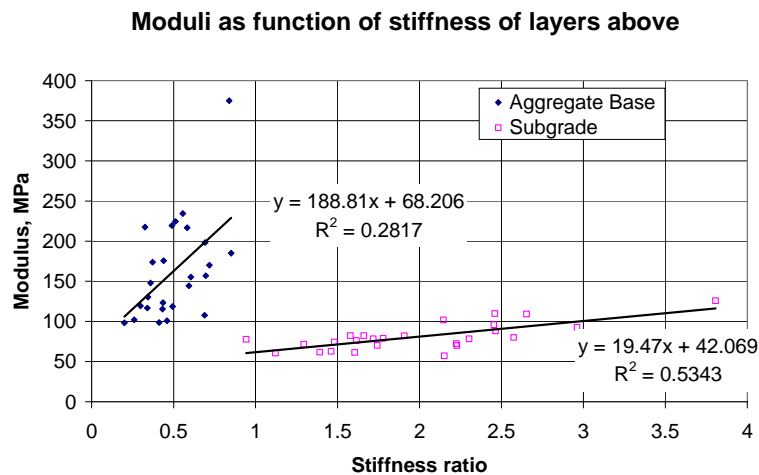
Figure 1 Correlation between moduli of unbound layers and stiffness ratio of layers above the layer considered (S/3500^3 in Equation 5), all sections.

The regression equations in Figure 1 results in the relationships:

$$E_{AB} = 257\,MPa \times \left(1 - \left[1 - \frac{S}{3500^3}\right] \times 0.73\right), R^2 = 0.28, SEE = 52\,MPa$$

$$E_{SG} = 62\,MPa \times \left(1 - \left[1 - \frac{S}{3500^3}\right] \times 0.32\right), R^2 = 0.53, SEE = 11\,MPa$$

Similar relationships were derived for the aggregate base of the individual test sections for the calibration of the incremental-recursive models of CalME. The subgrade modulus was assumed to be constant, for reasons explained below (see Figure 6).

The stiffness of the unbound layers was simultaneously modeled as a function of the load level. This is a well known non-linearity, with the modulus of granular materials increasing with increasing bulk stress and the modulus of the cohesive subgrade, common to all of the sections, decreasing with increasing deviator stress. Load level had to be used instead of stress because of the effects of confinement. During backcalculation of layer moduli the subgrade modulus was assumed to decrease with the load level raised to a power of -0.2.

All materials were assumed to have a Poisson's ratio of 0.35.

Damage to Asphalt Layers

The model for damaged asphalt concrete modulus was:

$$\log(E) = \delta + \frac{\alpha \times (1 - \omega)}{1 + \exp(\beta + \gamma \log(tr))}$$

Equation 6: Modulus of damaged asphalt concrete.

where the damage, ω, was calculated from:

$$\omega = A \times MN^{\alpha} \times \left(\frac{\mu\varepsilon}{200\ \mu strain}\right)^{\beta} \times \left(\frac{E}{3000\ MPa}\right)^{\gamma} \times \left(\frac{E_i}{3000\ MPa}\right)^{\delta}$$

Equation 7: Damage as a function of load applications, strain, modulus and temperature.

where *MN* is the number of load applications in millions,
$\mu\varepsilon$ is the tensile strain at the bottom of the asphalt layer,
E is the modulus,
E_i is the modulus of the intact material, and
A, α, β, γ, and δ are constants (not related to the constants of Equation 6).

Equation 6 leads to:

$$\log(E) - \delta = (\log(E_i) - \delta) \times (1 - \omega), \text{ or}$$

$$\frac{E}{E_i} = \left(\frac{E_{\min}}{E_i}\right)^{\omega}, \text{ or}$$

$$\omega = \frac{\log\left(E/E_i\right)}{\log\left(E_{\min}/E_i\right)} = \frac{\ln(SR)}{\ln\left(E_{\min}/E_i\right)}$$

Equation 8. Relations between moduli and damage.

where SR is the stiffness ratio
Damage is sometimes defined as the relative decrease in modulus, *(E$_i$ – E)/E$_i$ = dE/E$_i$*. The MEPDG defines damage both through Equation 6 and as the relative decrease in modulus. These two definitions of damage are incompatible with each other. If damage is defined through Equation 6 then the relative

decrease in modulus will depend on the minimum modulus, E_{min}, and on the initial modulus, E_i, which again is a function of temperature and loading time.

The constant γ was assumed to equal $\beta/2$, making damage a function of the internal energy density. The parameters of Equation 7 were determined from four point beam, controlled strain, fatigue testing, by minimizing the Root Mean Square (RMS) of the difference between the measured modulus and the modulus calculated from Equation 6. Moduli below 30% of the intact value were not included, because the laboratory tests at this amount of damage are unlikely to be representative of the in-situ conditions of an asphalt layer. The minimization was done in Excel using Solver.

Strain 407 µm/m

Strain 383 µm/m

Strain 413 µm/m

Strain 211 µm/m

Stain 198 µm/m

Strain 211 µm/m
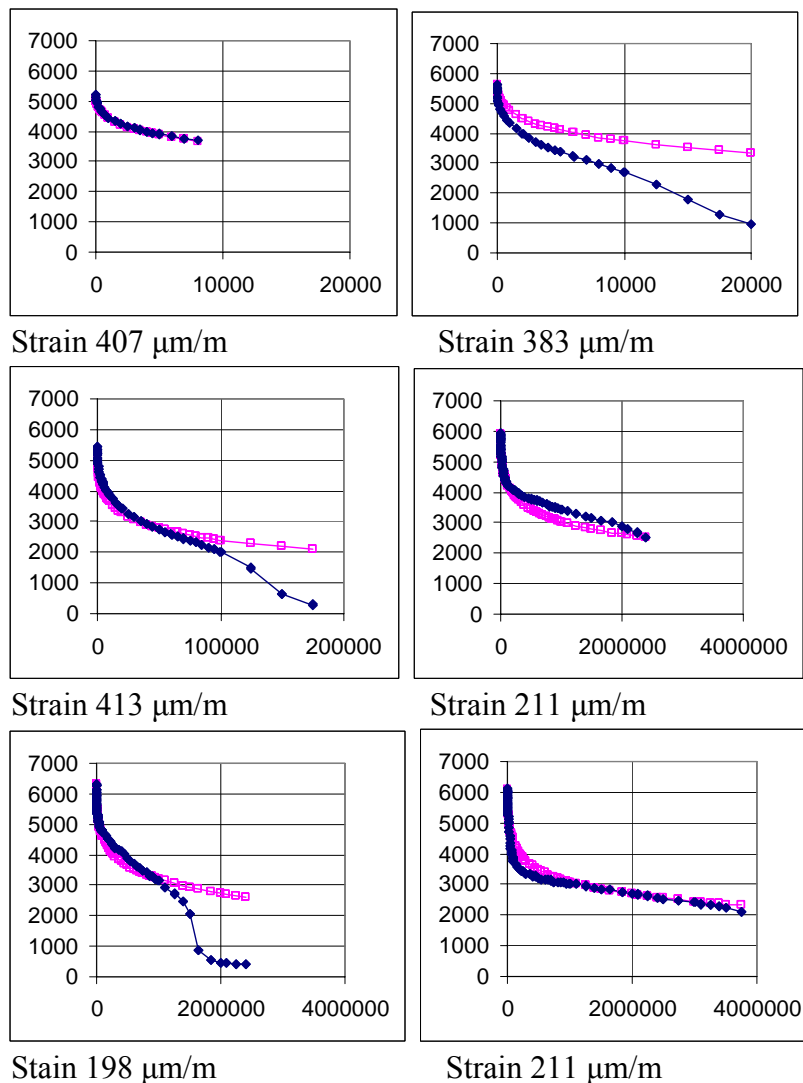
Figure 2 Example of laboratory fatigue tests from section 02FML, 20 ºC.

An example from section 02 is shown in Figure 2. The ordinate is the modulus in MPa and the abscissa is the number of load applications. The measured moduli are shown as a filled diamond signature (blue) and the values determined from Equation 6 are shown as open squares (magenta). The average strain during the fatigue test is given below each graph.

The parameter δ in Equation 7 was based on the parameter for initial asphalt moduli in the Asphalt Institute criterion for asphalt fatigue. With this criterion the damage will be proportional to the initial modulus raised to -α times -0.854 (= 0.854×α). This results in positive values of δ, between 0.3 and 0.5.

Section 15FMM2 had fatigue tests at three different temperatures 5, 20, and 30 ºC. From these tests a value of δ = -1.9 may be derived for laboratory tests. This value is in good agreement with values determined for AC materials used during HVS tests, but it predicts that most damage in the pavement structure occurs at high temperatures. This was not a problem during the simulation of the HVS tests where all of the cracking tests were done at an almost constant temperature of 20 ºC.
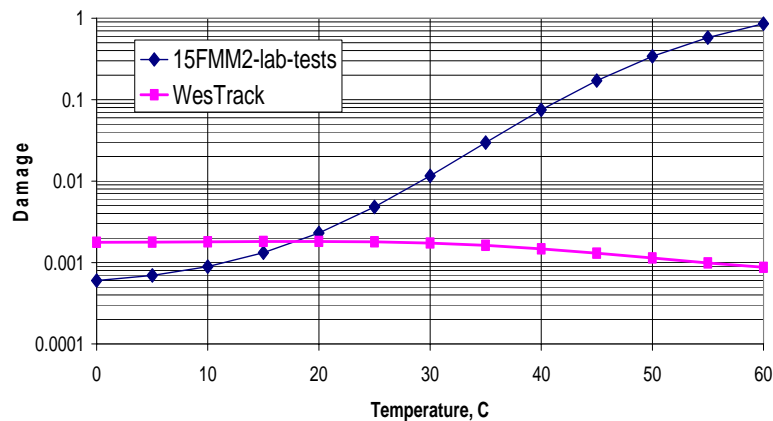
Figure 3 Damage at 200 load applications calculated for laboratory value of δ and value used in WesTrack simulation.

Figure 3 illustrates the problem. In this figure damage has been calculated both for the fatigue relationship derived from the laboratory tests on section 15FMM2, with δ = -1.9306 and for the relationship used in the simulations of WesTrack with CalME, where δ was 0.3788 for section 15FMM2. The master curve determined for section 15FMM2 is used for the modulus of the AC layer in the calculations. A 150 mm thick AC layer resting on a granular base with a modulus of about 220

MPa was assumed. The structure was loaded by a 20 kN single wheel load with a tire pressure of 0.7 MPa. The tensile strain at the bottom of the AC layer was calculated using Odemark-Boussinesq's approach, and the damage was accumulated using the incremental-recursive procedure. The figure shows the accumulated damage after 200 load applications, at different temperatures (the temperature being kept constant during the 200 load applications).

The maximum temperatures at the WesTrack experiment were close to 60 ºC. At this temperature 200 load applications (of a 20 kN load) would lead to complete failure, with a damage value close to 1. This creates two problems:

- One is that a very high lab to field shift factor must be used (a value of several hundred) in order to avoid that the simulations result in premature failure of the sections. Such a high shift factor is unreasonable when compared to the simulations of the HVS tests where a factor of 3 was found.
- The other problem is that the modulus at the reference temperature would decrease during the warm seasons, according to the laboratory values. This is contrary to the change in moduli determined from FWD tests, which show a decrease in modulus at the reference temperature during the cold seasons (see Figure 15).

Because of these problems the value of δ in the damage relations was determined as described above. It should be noticed that the stress conditions at the bottom of an asphalt layer at very high temperatures are quite different from those of a fatigue beam in the laboratory. In the laboratory test the first stress invariant is always tensile whereas the first stress invariant at the bottom of an asphalt layer will change with temperature and may become compressive at high temperatures. The fatigue models in the MEPDG and the Asphalt Institute fatigue model also predict that most pavement damage occurs at the highest temperatures.

Permanent Deformation of Asphalt

A shear-based approach, developed by Deacon et al. (8), for predicting rutting of the asphalt layer was used. Rutting in the asphalt is assumed to be controlled by shear deformation. The

permanent, or inelastic, shear strain, γ^i, is determined from Repeated Simple Shear Tests at Constant Height (RSST-CH) in the laboratory as a function of the shear stress, τ, the elastic shear strain, γ^e, and the number of load repetitions. The best fitting relationship for the materials used was found to be a power function:

$$\gamma^i = A \times MN^\alpha \times \exp\left(\beta \times \tau / \tau_{ref}\right) \times \gamma^e$$

Equation 9 Power function for permanent shear strain.

where γ^e is the elastic shear strain,
      τ is the shear stress,
      MN is the number of load repetitions in millions,
      τ_{ref} is a reference shear stress (0.1 MPa), and
      A, α, and β are constants determined from the RSST-CH.
      A constant value of 1.03 for β, determined from previous work (8), was used for all materials. The rest of the parameters were determined by minimizing RMS of the difference between the measured shear strain and the strain calculated from Equation 9.
      The rut depth is calculated for the upper 100 mm of the AC layers. The shear stress is calculated at a depth of 50 mm beneath the edge of the tire. For each of the layers within 100 mm from the surface the elastic shear strain, γ^e, is calculated from:

$$\gamma^e = \frac{\tau}{E_i / (1 + v_i)}$$

Equation 10 Calculation of elastic shear strain in top layers.

where E_i is the modulus of layer i, and
      v_i is Poisson's ratio for layer i (0.35 used here).

The permanent shear strain of each layer is calculated from Equation 9, and the permanent deformation is determined from:

$$dp_i = K \times h_i \times \gamma^i$$

Equation 11 Relationship between permanent deformation and permanent shear strain of layer i.

where h_i is the thickness of layer i (above a depth of 100 mm),
and
K is a calibration constant.

The AC layer was subdivided into three layers in the layer elastic calculation of elastic shear stress and strain to include the effects of temperature gradients on the mix stiffness, with thicknesses from top to bottom of 25 mm, 50 mm and the remaining AC thickness as the third layer.

The total permanent deformation in the AC is the sum of the permanent deformations of the layers within the top 100 mm of the AC. A value of $K = 0.9$ was used for all the Fine and Fine Plus mix materials and of $K = 0.8$ for the Coarse mixes.

The average decrease in air voids over the first 12 months of the experiment, ΔAV, for the top and bottom lifts combined based on measurements from cores, was found to be:

$$\Delta AV = 0.36 \times AV_{original}$$

Equation 12 Average decrease in air voids.

This decrease was used in the simulations with CalME. It was assumed to occur over the first 60 days with traffic loading, and was distributed over the asphalt layers, proportional to the thickness of the layers. This last assumption may result in too large a contribution from the bottom layer.

Permanent Deformation of Unbound Layers

The model for permanent deformation of the unbound layers, dp, is given in Equation 13, where MN is the number of load applications in millions, $\mu\varepsilon$ is the vertical compressive resilient strain at the top of the layer and E is the modulus. The relationship was derived from tests in the Danish Road Testing Machine during the International Pavement Subgrade Performance Study (9):

$$dp\ mm = A \times MN^{\alpha} \times \left(\frac{\mu\varepsilon}{1000\ \mu strain}\right)^{\beta} \times \left(\frac{E}{40\ MPa}\right)^{\gamma}$$

Equation 13: Permanent deformation of unbound layers.

A was 0.8 mm for aggregate base and 1.1 mm for subgrade. $\alpha = 0.333$, $\beta = 1.333$ and $\gamma = 0.333$ were used for both layers. These are the same values used for HVS calibration (2).

Roughness

Roughness was measured in both of the wheel paths in terms of the International Roughness Index (IRI). In CalME simulations of Westrack the increase in IRI, *ΔIRI*, was predicted from a simple subgrade strain model (9):

$$\Delta IRI \, m/km = A \times MN^{\alpha} \times \left(\frac{\mu\varepsilon}{1000 \, \mu strain}\right)^{\beta} \times \left(\frac{E}{40 \, MPa}\right)^{\gamma}$$

Equation 14 Roughness model for subgrade.

where $\mu\varepsilon$ is the elastic vertical compressive strain at the top of the subgrade and
 E is the modulus of the material.
 The parameters used were $A = 0.64$ m/km, $\alpha = 0.333$, $\beta = 1.333$ and $\gamma = 0.333$. The measured roughness was very irregular, with values sometimes increasing or decreasing dramatically. The values predicted by Equation 14 were not unreasonable, but a rigorous calibration was not possible.

Time Hardening Procedure

The models described above are used in an incremental-recursive process. This means that the parameters on the right side of the equal-sign may change from increment to increment. The first step in the process is, therefore, to calculate the "effective" number of load applications that would have been required, with the present parameters, to produce the condition at the beginning of the increment. This sometimes requires an iterative procedure. In the second step, the new condition at the end of the increment is calculated for the "effective" number of load applications plus the number of applications during the increment. This must be repeated for each load and load position during the increment.

The method may be illustrated by an example using Equation 13. If, for example, the permanent deformation of the subgrade was 2 mm at the start of an increment, the vertical

strain calculated for the first wheel load at the first position was 800 μstrain and the modulus 60 MPa. Then the "effective" number of load applications at the start of the increment may be found from:

$$MN_{eff} = \left[\frac{2}{1.1 \times \left(800/1000\right)^{1.333} \times \left(60/40\right)^{0.333}} \right]^{1/0.333}$$

If the number of repetitions, in millions, of this load, at this position, was *dMN* during the increment, then the permanent deformation after these load applications would be:

$$dp, mm = 1.1 \times \left(MN_{eff} + dMN\right)^{0.333} \times \left(800/1000\right)^{1.333} \times \left(60/40\right)^{0.333}$$

The process must be repeated recursively, using the output from each calculation as input to the next, for all loads at each position, before proceeding to the next time increment.

Calibration of Incremental-Recursive Models

A wander pattern was applied at WesTrack, but not until the rutting exceeded 6 mm on most sections. It was observed that once the rut depth exceeded 6 mm it tended to guide the wheels so that the trucks tracked the same line with little or no wander. In addition there were some uncertainties as to the actual lateral positions of the wheels. A wander pattern was, therefore, not applied in the simulations. The vehicle speed was 64 km/h.

Asphalt Moduli

Asphalt moduli were obtained from a number of different test methods. The largest amount of data was from backcalculation of FWD tests done during the experiment. The backcalculation of layer moduli was done using the program Elmod5 (10) with a constant non-linearity of -0.2 for the subgrade, as mentioned above. Backcalculations were done for all of the FWD test series, and for the test positions between the wheel paths and in the right wheel path.

Indirect tensile tests were done at "Time Zero Construction" (September 1995), "Time Zero Traffic", "12 Months Traffic" and "Post Mortem", for some of the sections. The moduli were measured at 25 ℃ with a 0.1 sec haversine load pulse, but were converted to the reference temperature of 15.4 ℃ and 15 msec load pulse duration (corresponding to the FWD load).

The increase in moduli during the experiment was sometimes very large, in some cases showing a doubling of the modulus. An increase in modulus caused by aging of the binder would be expected to be most pronounced shortly after construction, but there is no increase in modulus from "Time Zero Construction" to "Time Zero Traffic". This would indicate that most of the hardening is due to decrease in air voids caused by post compaction. Comparison of values at "12 Months Traffic" and "Post Mortem" also indicates that the hardening of the asphalt occurred within the first 12 months of trafficking.

RSST-CH tests on the original asphalt and after trafficking (post mortem) confirm the large increase in modulus during the experiment. The ratio between the hardened shear modulus (Gpm) and the original shear modulus (Go) is shown in Table 1 for the Fine mix. The hardening is quite similar to what was found from the indirect tensile tests.

Table 1 Hardening from shear tests, Fine mix

Mix	Gpm/Go
LH	2.59
LM	1.72
MH	2.73
MM	1.90
ML	1.16
HM	2.03
HL	0.55

Frequency sweep tests on beams were carried out, but only for one sample for each of the Fine, Coarse and Fine Plus mixes. Shear frequency sweep data were also available for a few of the test sections, at 10 Hz and temperatures of 40, 50 and 60 ℃. Initial moduli were also derived from fatigue tests on beams. Five to six specimens were available for each test section.

Figure 4 compares the asphalt moduli determined by different experiments for section 18FHL, which had little hardening and no cracking during the experiment. Equation 14 from Chapter 4 of (3) was also used in the comparison. An

asphalt content of 6.2% and an air voids content of 4.3% were used. Different sources give different values for the air voids content but 4.3% appears to be a reasonable value, for section 18, at the start of the test (dropping to about 2.1% towards the end of the experiment).

The legends are: "Mr HL" – initial resilient modulus from indirect tensile tests (UNR), "FS UCB" flexural frequency sweep data from UCB, "Fatigue HL" – moduli from fatigue beams (UCB), "FS FHWA" – shear frequency sweep data from FHWA, "Table 2.3" – FWD backcalculated moduli from the UCB report (4), "Eq 14-18" – from the NCHRP report (3), with asphalt content and air voids for section 18, "FWD" – moduli backcalculated with Elmod5 and "FWD-age" the same moduli adjusted for the effects of hardening. The curve "Model" was the best estimate using Equation 1.

Using the MEPDG procedure with the volumetric data for section 18 resulted in a very low minimum modulus (10^{δ}) of 8 MPa and a maximum modulus ($10^{\alpha+\delta}$) of more than 110,000 MPa. Both of these values are unrealistic, and the MEPDG master curve does not compare very well to the measured moduli, as seen in Figure 5.
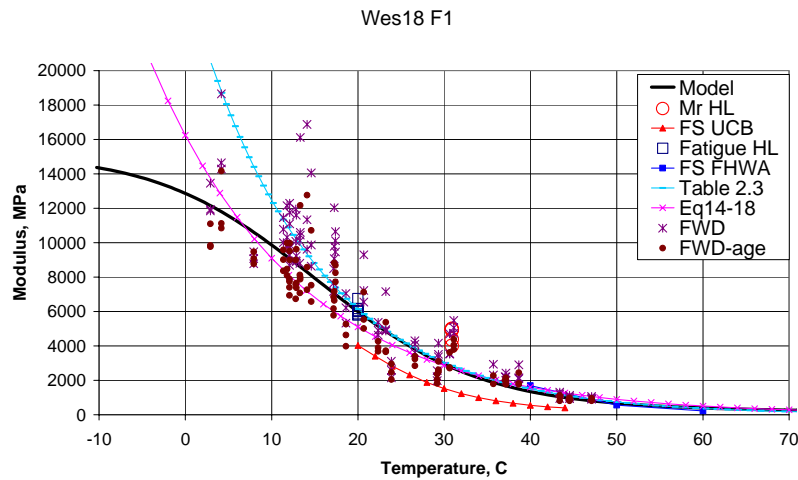
Figure 4 Asphalt modulus as a function of temperature.

An older version of the MEPDG master curve was given by Witczak & Fonseca (11). This version is also shown in Figure 5 and fits the measured data better than the master curve estimated from volumetric data following the MEPDG procedure.

Wes18 F1
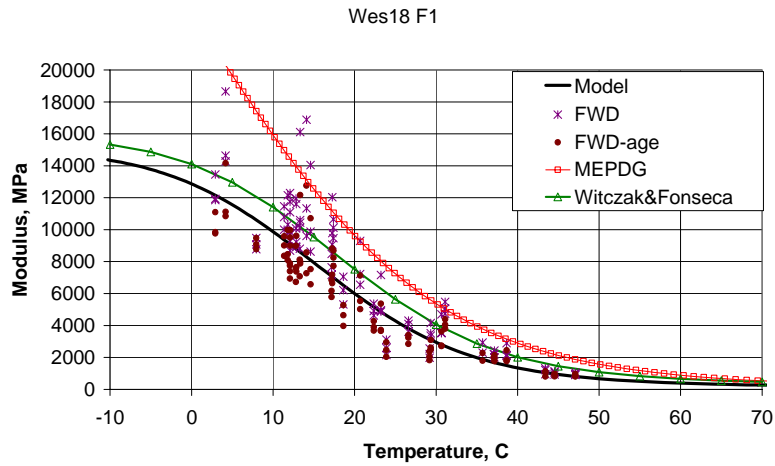
Figure 5 Section 18 Best fit "Model" master curve compared to master curve estimated from volumetric data following MEPDG.

Unbound Layer Moduli

Backcalculated Moduli

Stiffness factors were calculated for the granular layer for the individual sections as described above. For the subgrade the modulus was assumed to remain constant, even though it did show some dependence on the stiffness of the pavement layers for some sections and a variation that was probably associated with flooding of the Carson River for other sections, as shown in Figure 6. A variation of subgrade modulus like the one shown in Figure 6 cannot presently be handled by CalME.

Subgrade modulus
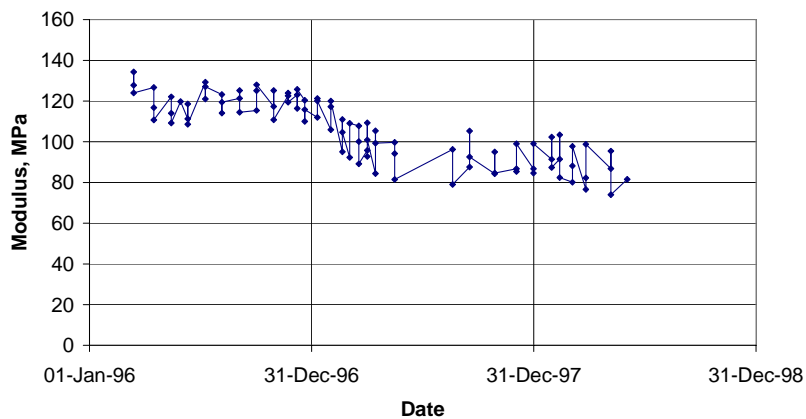
Figure 6 Variation of subgrade modulus with time for section 18.

Moduli from triaxial tests

Triaxial tests were available for the Aggregate Base and for some of the Engineering Fill lifts, but only for some of the test sections. For the Aggregate Base, the triaxial modulus was primarily a function of the bulk stress, $\theta = \sigma_1 + \sigma_2 + \sigma_3$, with the shear stress (or deviator stress) having very little effect on the modulus. The modulus could be calculated from:

$$Eab = 206\,MPa \times \left(\frac{\theta}{0.1\,MPa} \right)^{0.64}$$

Equation 15 Modulus of Aggregate Base from triaxial tests.

The agreement between the modulus measured in triaxial tests and the modulus calculated from Equation 15 is shown in Figure 7.

Modulus of Aggregate Base
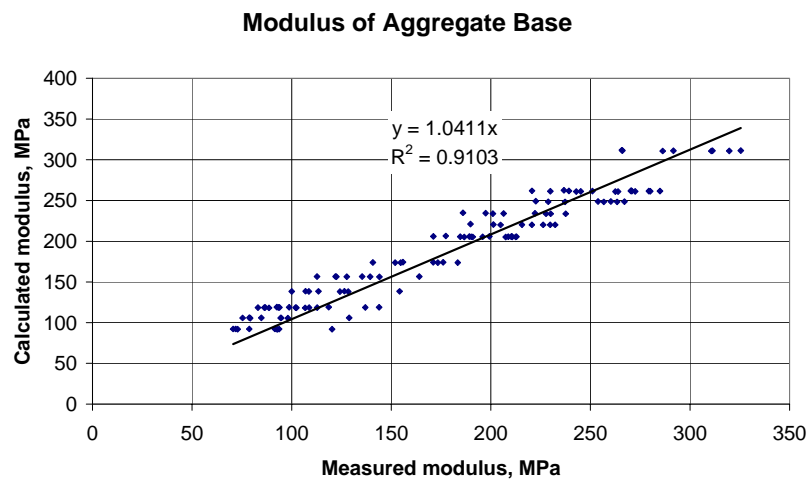
Figure 7 Moduli calculated from Equation 15 **versus moduli from triaxial tests.**

For the Engineering Fill the variation was very large from section to section, as shown in Figure 8 where the modulus is shown as a function of the deviator stress and the vertical differences (within a test section) are due to differences in confining stress. It can be seen that the deviator stress can both cause an increase and a decrease in the modulus. It was not possible to describe the modulus by a single relationship.

Examples of triaxial tests on Engineering Fill
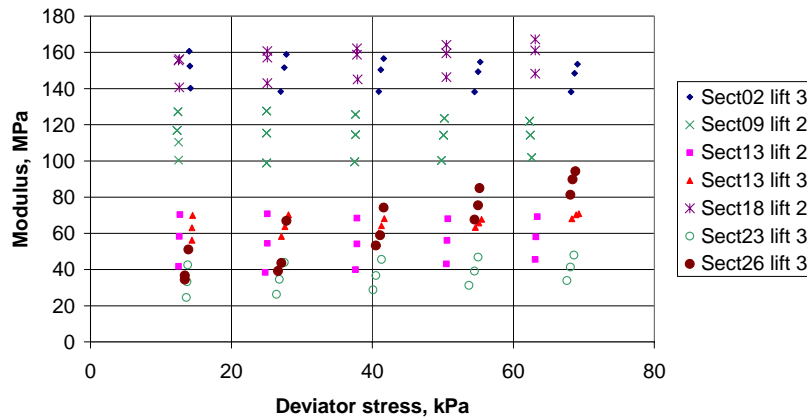
Figure 8 Examples of triaxial tests on Engineering Fill, at varying confining and deviator stresses.

To relate the triaxial test results to the moduli under truck loading, the bulk stress was calculated for the duration of the test for section 18 using CalME. The bulk stress was calculated at a depth of 50 mm below the Aggregate Base (AB) and the same depth below the top of the Subgrade (SG, Engineering Fill), see Figure 9.

For the Aggregate Base, the bulk stress was used to calculate the modulus for the duration of the test, using Equation 15.

Bulk stress in unbound layers, 50 mm below surface of the layer
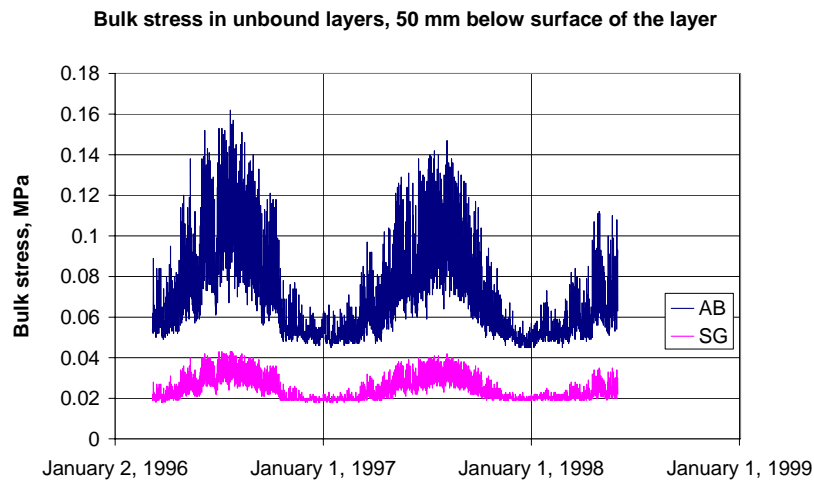
Figure 9 Bulk stress in Aggregate Base and in Subgrade, 50 mm below the surface of the layers, section 18

Figure 10 shows the modulus of the AB, as calculated from the bulk stress using Equation 15 for triaxial tests and as determined from backcalculation of FWD data. During cold periods where the asphalt layer is stiff the bulk stress in the AB is low, resulting in a low triaxial modulus. The opposite is true for the FWD moduli.

Modulus of Aggregate Base
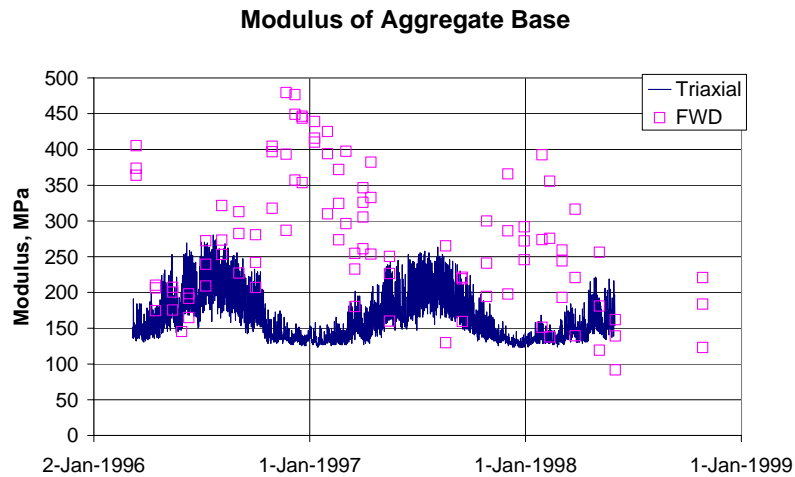
Figure 10 AB moduli at test section 18, from triaxial tests and FWD.

Figure 11 compares the moduli calculated by CalME, using the stiffness function in Equation 5, to the moduli backcalculated from FWD testing. It is obvious that use of the stiffness function results in a much better agreement with moduli backcalculated from FWD testing than use of the bulk stress relationship derived from triaxial testing.

Modulus of Aggregate Base
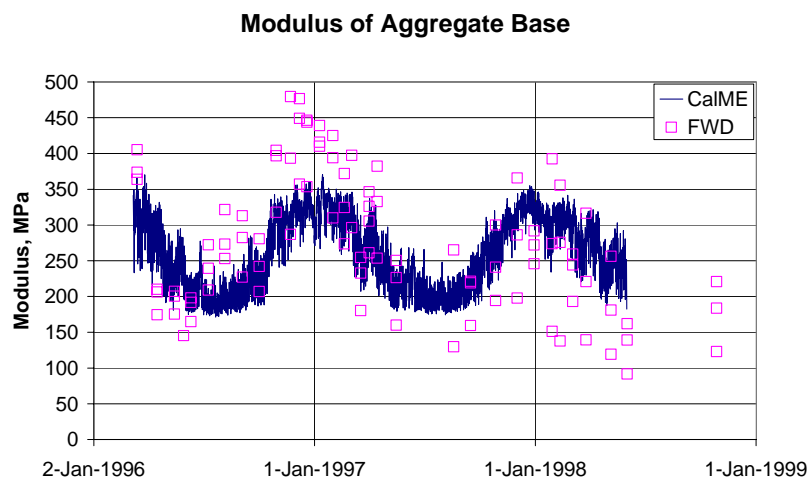
Figure 11 AB moduli calculated by CalME compared to FWD determined moduli.

Figure 12 shows the moduli of different lifts of the Engineering Fill, as determined from triaxial testing at a bulk stress of 30 – 40 kPa, which is on the high side of the actual bulk stress. The moduli from the first FWD tests in March 1996 are shown as a comparison. The average modulus from triaxial testing is 112 MPa, and 81 MPa from FWD tests. Multiplying the FWD derived subgrade modulus by a factor of 0.35, as recommended by the MEPDG, would clearly not be appropriate.

Modulus of Engineering fill
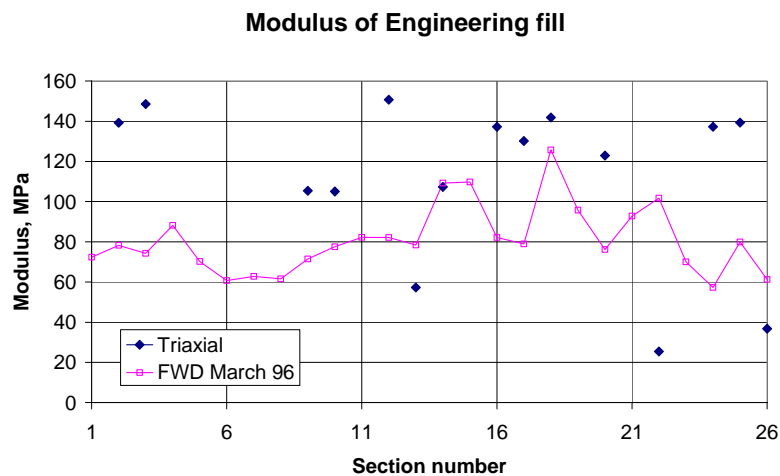
Figure 12 Modulus of Subgrade from triaxial tests and from FWD backcalculation.

Simulation of Pavement Response

The results from WesTrack were imported to the CalME database and the experiment was simulated, section by section, using a time increment of one hour and the measured temperatures and load applications during each hour. The only measured response available from WesTrack was the FWD deflections. Figure 13 shows the FWD deflection at the center of the loading plate in the wheel path (F3) as a function of time, for section 18. The deflections correspond to a peak load of approximately 40 kN (the actual load level was used both for measured and calculated values). The legends marked "M" are the measured values. The measured points are connected by fully drawn lines. The corresponding calculated deflections have legend "C" and the points are connected by dotted lines. Figure 13 shows results from four FWD positions within Section 18.

"35_1" in the header of the figure indicates a test point between chainage 30 m and 39 m.
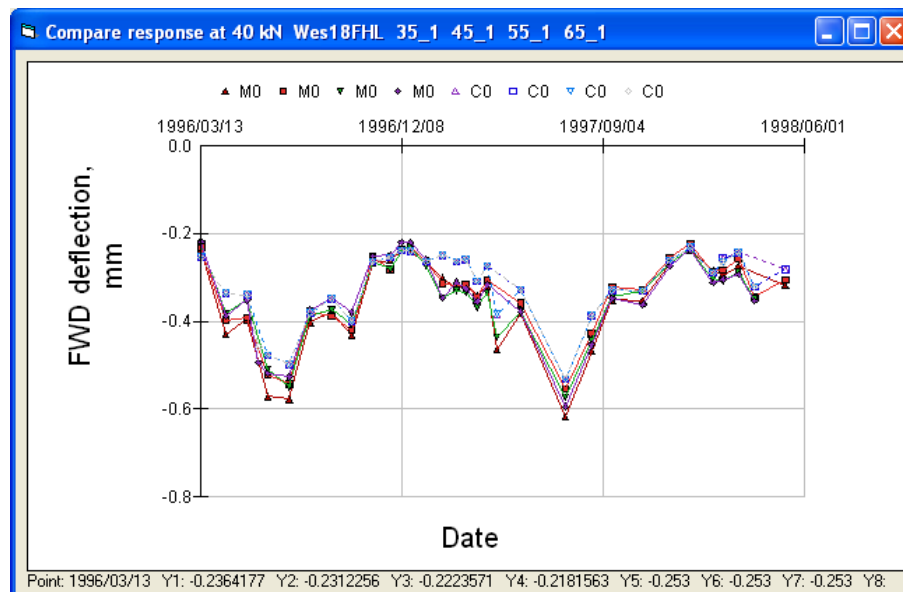
Figure 13 FWD deflections at section 18 (in wheel path, geophone under the loading plate).
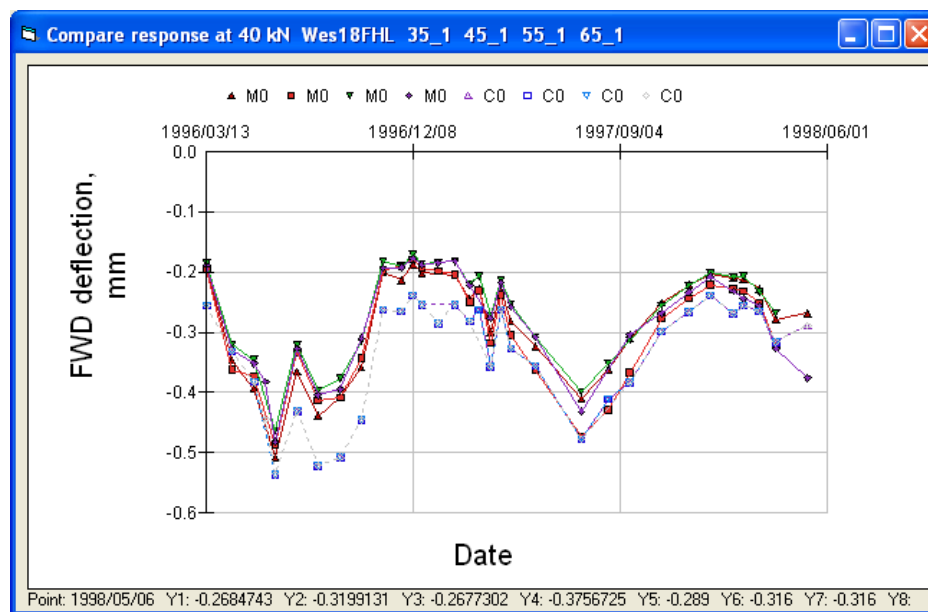

Figure 14 FWD deflections at section 18 (between wheel paths, geophone under load plate).

The agreement between the measured and the calculated deflections is seen to be very good in this case. The mean difference between the four measured deflections in Figure 13 is

2 µm (10^{-6} m) and the Root Mean Square (RMS) difference is 55 µm. The mean difference between measured and calculated deflections is 3 µm and the RMS is 33 µm.

Figure 14 shows the measured deflections between the wheel paths, compared with the calculated deflections based on the damaged asphalt in the wheel path (calculated deflections are identical to the calculated deflections of Figure 13). The figure clearly shows that the asphalt in the wheel paths did suffer some damage, resulting in larger deflections, even though no visible fatigue cracking was recorded on this section.

Simulation of Damage

Wes16 in wheel tracks
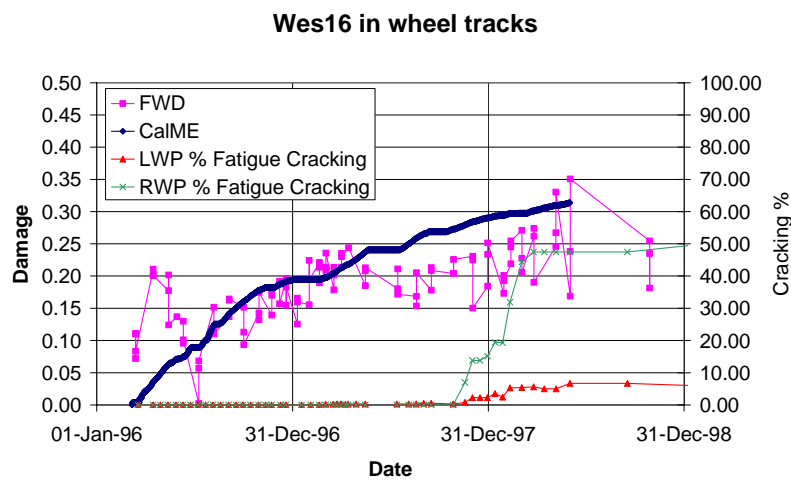
Figure 15 Damage in wheel path of section 16 (LWP = left wheel path, RWP = right wheel path).

The progression of damage influences the change in pavement response, so the simulation of response and damage are mutually dependent. Section 18 which had no cracking and very little simulated damage is not very illustrative. On the other hand, Section 16FLH2 had a few percent cracking in the left wheel path (LWP) and about 50 % in the right wheel path (RWP), at the end of the experiment.

Figure 15 shows the damage parameter, ω, from Equation 7 on the left y-axis, as simulated by CalME and as estimated from the FWD tests on section 16, both are from the right wheel path. The FWD moduli were adjusted for temperature and hardening and any remaining difference between the backcalculated values and the master curve was

assumed to be due to damage. On the right y-axis is shown the recorded cracking.

Simulation of Permanent Deformation

To obtain a reasonably good agreement between the permanent deformation calculated with CalME and the measured down rut, a value of K = 0.9 (in Equation 11) was used. (Note that K should be multiplied by 100 in order to compare to the K value used by Deacon et al., (8). They reported a K value of 140 for an asphalt thickness of 150 mm increasing to 250 for a thickness of 300 mm, but this included the post compaction which is treated separately here.) For the Coarse sections K was equal to 0.8. As mentioned above, a post compaction corresponding to 36% of the air voids content was assumed to take place within the first 60 days with traffic loading.

Figure 16 shows the down rut in the right wheel path of Section 18. Again, measured values are connected by a fully drawn line whereas the values calculated by CalME are connected by a dotted line.
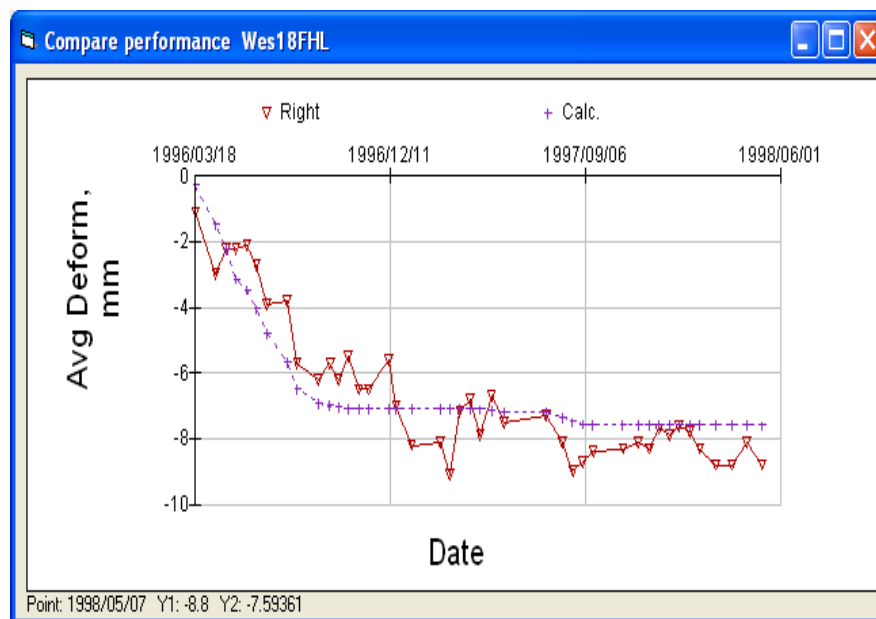
Figure 16 Down rut in right wheel path at section 18.

In Figure 16 the mean difference between the measured down rut depth and the calculated permanent deformation is

0.9 mm and the RMS is 1.3 mm. Figure 17 shows the simulation results compared to the measured maximum rut depths (the distance from the highest peak of the rut to the bottom of the rut) in the right and left wheel paths. The mean difference between rutting in the left and the right wheel path in Figure 17 is 2.7 mm and the RMS is 4.0 mm.

The maximum rut depth in the right wheel path, shown in Figure 17, is not much different from the down rut shown in Figure 16, whereas the rutting in the left wheel path is larger.
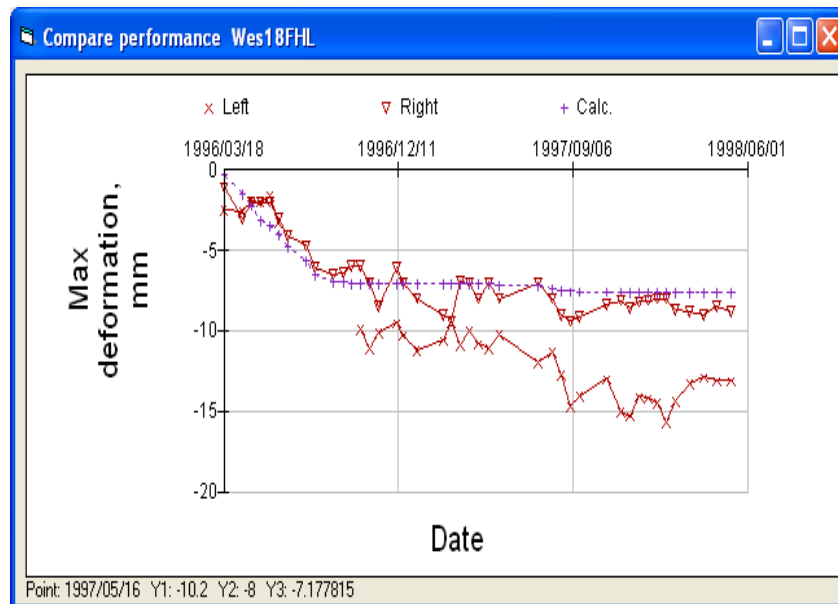
Figure 17 Maximum rutting in left and right wheel paths at section 18.

Summary of Analyses and Conclusions

Deflection Response

The agreement between the measured and calculated response during the duration of the Westrack trafficking on each section, in terms of the deflection under the load plate of the FWD, was very good in most cases. The calculated deflection is a function of the following factors which are considered in CalME:

- the estimated asphalt temperature during the FWD test,
- the asphalt modulus versus reduced time relationship,
- the moduli of the unbound materials (aggregate base and subgrade),

- the hardening of the asphalt material as a function of post compaction and ageing, and
- the damage to the asphalt caused by fatigue.

The measured deflections will be a function of the actual asphalt temperature during the FWD tests, the contact between the FWD loading plate and the pavement surface as well as of the position of the test.

Average FWD center deflection Fine mix
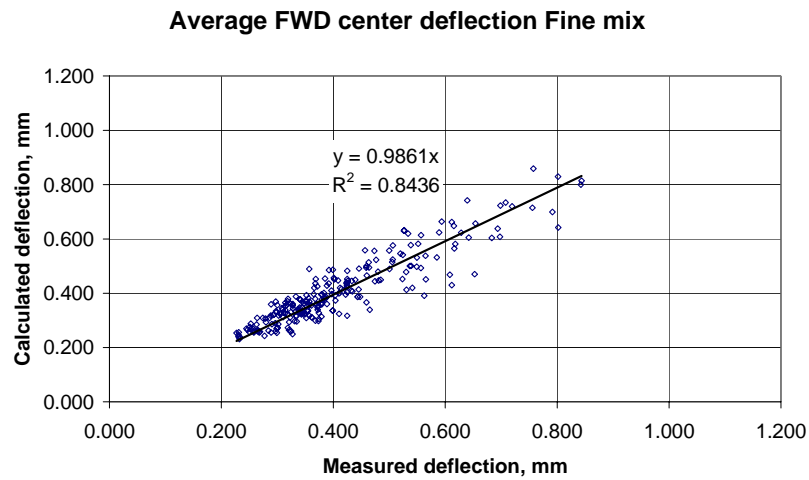
Figure 18 Measured and calculated center deflections on Fine mix sections

Average FWD center deflection Coarse mix
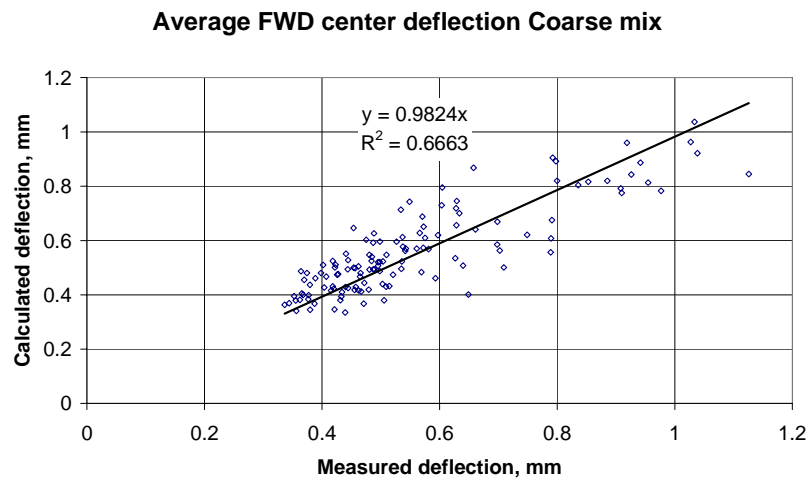
Figure 19 Measured and calculated center deflections on Coarse mix sections.

Average FWD center deflection Fine Plus mix

$y = 1.0167x$
$R^2 = 0.7901$
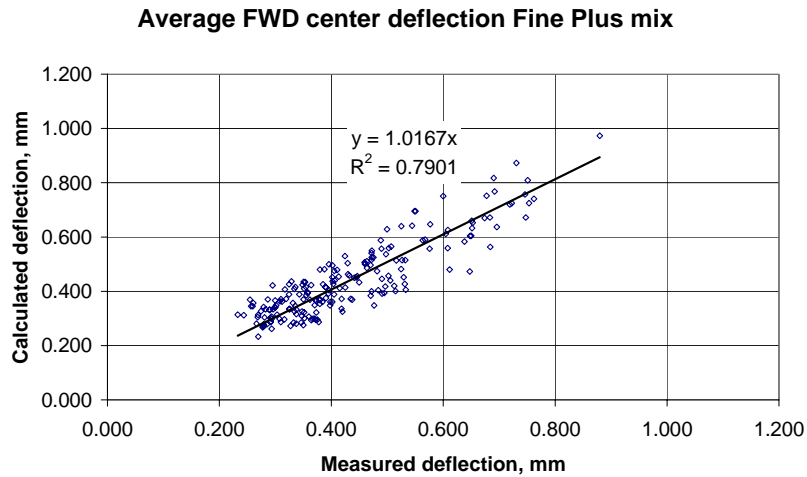
**Figure 20 Measured and calculated center deflections on Fine
Plus mix sections.**

Figure 18 to Figure 20 show the average deflection at the
center of the FWD loading plate, calculated for each section and
each monitoring session. Only tests done at a chainage of 30 m
or higher were used, in order to avoid the transition sections.

The standard error of estimate is 50 μm for the Fine mix
sections, 103 μm for the Coarse mix sections, and 60 μm for the
Fine Plus mix sections. For the Fine mix and the Fine Plus mix
these values are similar to the standard deviations of the
measured values for a single monitoring session on one test
section. In other words, the difference between measured and
calculated values is similar to the scatter in the measured values.
For the Coarse mix the standard error of estimate is somewhat
higher.

Average difference between measured and calculated deflection
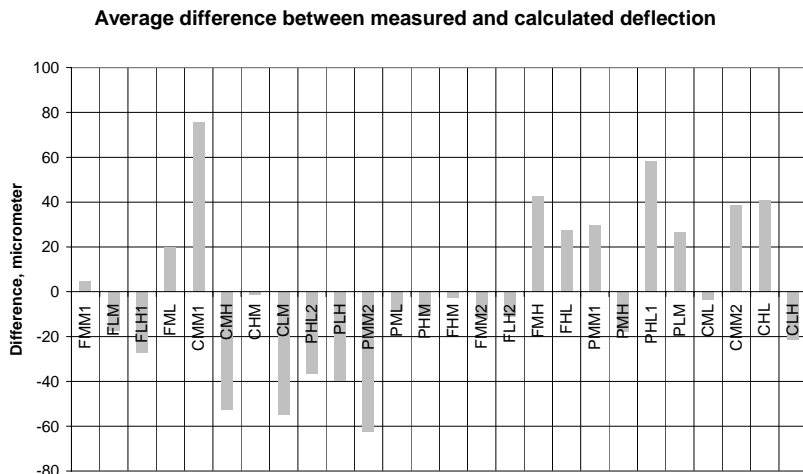
Figure 21 Deflection difference versus mix type.

Figure 21 shows the average difference between measured and calculated deflections in μm versus mix type. For comparison it may be noted that the average standard deviation on the measured deflections was 30 μm and the maximum average standard deviation for each section was 50 μm.

Figure 22 compares the Root Mean Square (RMS) differences between the measured deflections to the RMS differences between the measured and calculated values. The average RMS for the measured deflections is 45 μm and it is 65 μm for the difference between measured and calculated deflections.

Root Mean Square deflection difference, micron
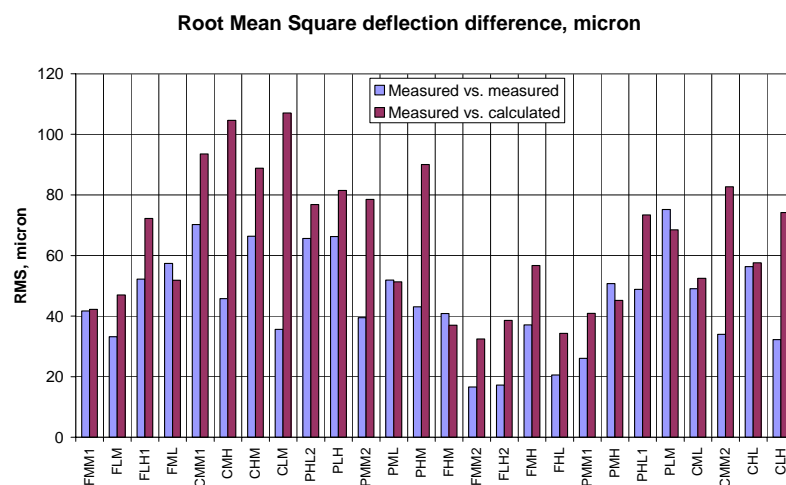
Figure 22 Comparison of RMS differences within measured and between measured and calculated response.

Relation of Cracking to Damage

Figure 23 compares the damage, ω, predicted by CalME based on the laboratory fatigue data, to the damage estimated from the FWD tests in the right wheel path. As explained above, the FWD backcalculated asphalt moduli were corrected for the effects of (estimated) temperature and hardening due to ageing and decrease in air voids content. The difference between the adjusted modulus and the modulus calculated from the modulus versus reduced time model was then assumed to be due to damage. Decrease in modulus was converted to damage using Equation 8.

On average, the Fine, Coarse and Fine Plus mixes all have less damage predicted by CalME than estimated from the FWD. The Coarse mix shows the largest difference, with the

FWD estimated damage being 2.2 times that of the CalME predicted damage, even though the shift factor used for the Coarse mix was 5, compared to 15 for the other two mixes. For the Fine and the Fine Plus mixes the ratio is 1.3 and 2.0, respectively. This indicates that the shift factors are too large, and that they are a function of mix type. This is quite reasonable as the influence of rest periods on the fatigue life is likely to be different for different mixes.

There is also some indication that mixes with a high binder content should have a lower shift factor than mixes with a low binder content, and that mixes with a low air voids content should have a lower shift factor than mixes with a high air voids content. This would indicate that the asphalt under in situ loading is less affected by the binder and air voids content than in the laboratory fatigue tests, but it should be recalled that the uncertainties on the damage estimated from the FWD tests are very large.
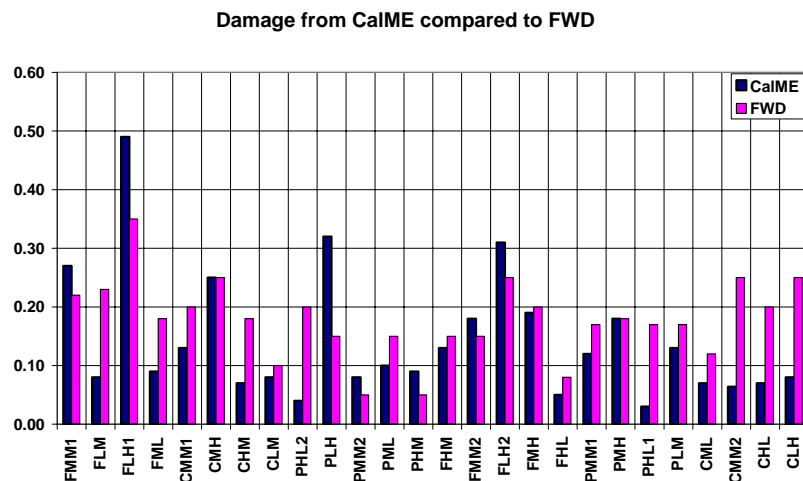

Figure 23 Damage predicted by CalME compared to damage estimated from FWD tests.

The cracking versus damage shown in Figure 24 also indicates that even the shift factor of 5 was too large for the Coarse mix. As noted above, the cracking is generally higher in the left wheel path than in the right wheel path, where the FWD tests were carried out.

Cracking % versus CalME damage
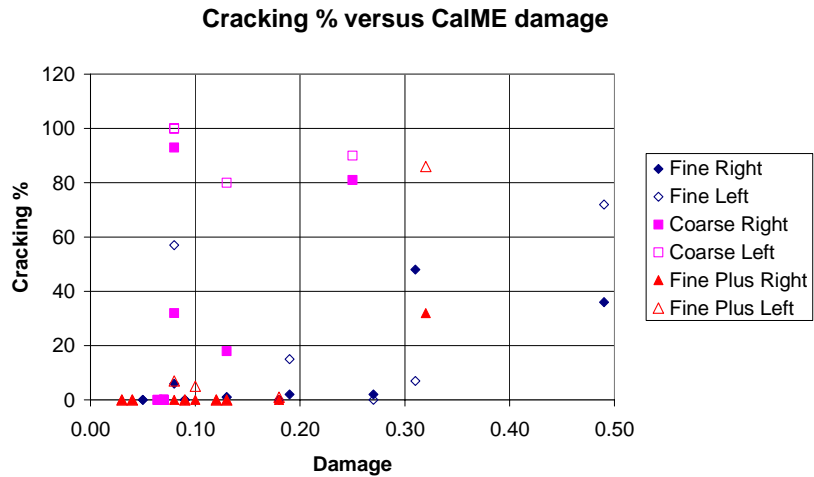
Figure 24 Cracking in left and right wheel paths as a function of damage predicted by CalME.

Permanent Deformation

Figure 25 shows the final permanent deformation calculated by CalME (for the right wheel path) and the maximum rutting recorded for the right and left wheel paths, which is not necessarily at the end of the experiment. The average values are: CalME 15.9 mm, 15.8 mm measured at right wheel path and 18.2 mm measured at left wheel path.

CalME deformation and maximum rutting
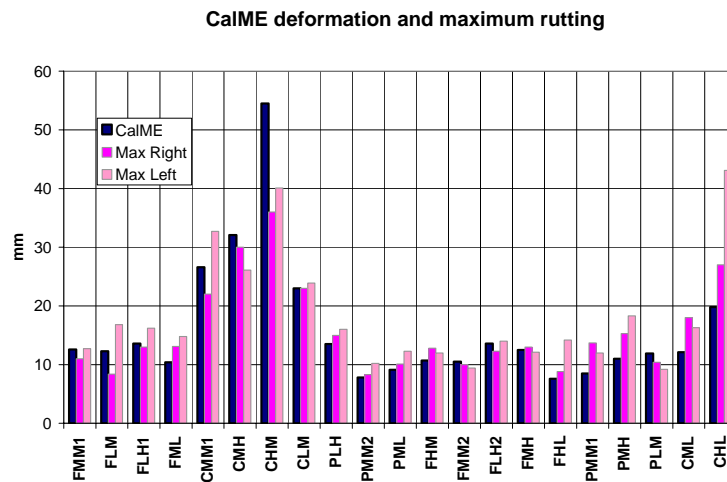
Figure 25 CalME deformation and maximum rutting in right and left wheel paths.

The main conclusions from the simulation of the WesTrack experiment with CalME are:

- The pavement response, in terms of resilient deflections, was predicted quite well, with the difference between measured and calculated values being similar to the scatter of the measured values, in most cases.
- The damage predicted by CalME, using laboratory fatigue tests, was somewhat lower than the damage estimated from the FWD tests. This indicates that the shift factors used in CalME should be reduced. The effect of temperature on damage needs further study.
- The permanent deformation predicted by CalME from RSST-CH testing in the laboratory was close to the measured rut depths.

Acknowledgement

References

1. NCHRP "Guide for Mechanistic-Empirical Design of New and Rehabilitated Pavement Structures". National Cooperative Highway Research Program, Report 1-37A, March 2004.
2. P. Ullidtz, J.T. Harvey, B.-W. Tsai, and C.L. Monismith, "Calibration of Incremental-Recursive Flexible Damage Models in CalME Using HVS Experiments". Report prepared for the California Department of Transportation (Caltrans) Division of Research and Innovation by the University of California Pavement Research Center, Davis and Berkeley. UCPRC-RR-2005-06. This and several related reports may be downloaded from http://www.its.berkeley.edu/pavementresearch/ Accessed July 2, 2007.

3. J. A. Epps, A. Hand, S. Seeds, T. Schulz, S. Alavi, C. Ashmore, C.L. Monismith, J.A. Deacon, J.T. Harvey, and R. Leahy, "Recommended Performance-Related Specification for Hot-Mix Asphalt Construction: Results of the WesTrack Project", Report 455, National Cooperative Highway Research Program, Transportation Research Board, Washington, DC, 2002.

4. C.L. Monismith, J.A. Deacon, and J.T. Harvey, "WesTrack: Performance Models for Permanent Deformation and Fatigue", Report to Nichols Consulting Engineers, Chtd., Pavement Research Center, Institute of Transportation Studies, University of California, Berkeley, 2000.

5. P. Ullidtz, J.T. Harvey, B.-W. Tsai, and C.L. Monismith, "Calibration of CalME Model Using WesTrack Performance Data". Report prepared for the California Department of Transportation (Caltrans) Division of Research and Innovation by the University of California Pavement Research Center, Davis and Berkeley. UCPRC-RR-200X-XX (under preparation).

6. P. Ullidtz, and P. Ekdahl, "Full-scale testing of pavement response", Proceedings, Fifth International Conference on the Bearing Capacity of Roads and Airfields, Vol. II, Trondheim 1998.

7. C.A. Richter. "Seasonal Variations in the Moduli of Unbound Pavement Layers". Publication No. FHWA-HRT-04-079, Federal Highway Administration, July 2006.

8. J.A. Deacon, J.T. Harvey, I. Guada, L. Popescu, and C.L. Monismith. "Analytically Based Approach to Rutting Prediction", Transportation Research Record 1806, Washington D.C., 2002.

9. P. Ullidtz. "Simple Model for Pavement Damage", Transportation Research Record, Journal of the Transportation Research Board, No. 1905, TRB, National Academies, Washington, D.C., 2005.

10. Dynatest http://www.dynatest.com/software/elmod_5.htm 2005

11. M.W. Witczak and O.A. Fonseca. "Revised Predictive Model for Dynamic (Complex) Modulus of Asphalt Mixtures", Transportation Research Record 1540, Transportation Research Board, 1996.